I&EC research
Industrial & Engineering Chemistry Research

Article

pubs.acs.org/IECR

# Spatial Reaction Engineering Approach (S-REA) as a Multiphase Drying Approach to Model the Heat Treatment of Wood under a Constant Heating Rate

Aditya Putranto[†,‡] and Xiao Dong Chen*[,†,‡]

[†]Department of Chemical Engineering, Monash University, Clayton Campus, Melbourne, Victoria 3800, Australia

[‡]College of Chemistry, Chemical Engineering and Material Science, Soochow University, Jiangsu Province, People Republic of China

[‡]Department of Chemical Engineering, Parahyangan Catholic University, Jalan Ciumbuleuit 94, Bandung, Indonesia

**ABSTRACT:** Wood may contain several harmful chemicals which can be removed by high-temperature treatment. This is essentially a drying process under linearly increased gas temperature up to final gas temperature of 220−230 °C which is a challenging process to model. The effective model is useful in process design, evaluation of equipment performance, and troubleshooting. In this study, the REA (reaction engineering approach) is implemented to describe the local evaporation/condensation rate and combined with a system of equations of conservation to yield a spatial model, called the spatial reaction engineering approach (S-REA), in order to model the heat treatment of wood under constant heating rate. A good agreement between the predicted and experimental data is observed. The REA is accurate to model the local evaporation rate of the heat treatment of wood. The S-REA is an effective nonequilibrium multiphase approach to model the heat treatment of wood, a simultaneous heat and mass transfer process involving water transformation under linearly increased gas temperature.

## 1. INTRODUCTION

Due to the presence of several harmful chemicals in wood including chromated copper arsenate (CCA), creosote, and pentachloro-phenol as a result of chemical processing, removal of the harmful chemicals are necessary.[1,2] Several methods for the removal could be conducted including recycling and recovery, chemical extraction, bioremediation, electrodialytic remediation, and thermal destruction.[2] Reuse and recycle may contaminate people handling the process since the process requires sorting, transportation, and storage. Chemical extraction has disadvantages of low kinetics and requirement of a multistep process. Remediation may result in loss of the quality of fiber. In addition, thermal destruction offers significant reduction in volume but evaluation and optimization are still required.[2] The thermal destruction can be conducted by a high-temperature treatment process in which wood samples are exposed in hot gas with linearly increased temperature up to temperatures above 200 °C. It is essentially a drying process under linearly increased gas temperature according to the heating rate.[1]

The heat treatment of wood is capable to enhance its quality since it can be applied to modify its dimensional stability, durability, and physical properties. Upon treatment, the color of wood changes and the color become uniform along the thickness.[3,4] The other properties including enhanced weather resistance, better decay resistance, and reduced shrinkage and swelling can also be improved by the thermal treatment.[5,6] The destruction of the hemicellulose seems to be the main cause of the change of properties. The changes start at temperature of 150 °C, and it continues as the temperature increases. During the wood heating, acetic acid is formed via hydrolysis of acetylated hemicellulose. The acid serves as catalyst for further hydrolysis of soluble sugars. The breaking of hemicellulose seems to be responsible for the reduction of generation of stress and increase of pressability of wood.[7] Thermal treatment of wood results in depolymerization because of cleavage of $\beta$-aryl-ether linkages and recondensation reactions related to formation of biphenolic and diarylmethane structures.[8] Upon heat treatment, it was found that the content of arabinose, manose, and galactose decreases.[9] The improved wettability was reported due to plasticization of lignin as a result of the decrease of water content,[10] while the improved color stability was analyzed due to the increase of lignin content.[11]

The heat treatment of wood has currently adopted by wood industry in Finland, France, and Germany by implementation of Thermowood Technology.[7] The process can be divided into three major steps. The first step is preliminary warming up to about 100 °C followed by steady increase to 130 °C up to 48 h. This is followed by another steady increase to 240 °C and holding the temperature constant at 240 °C for around 4 h. The last step is cooling and stabilization for up to 24 h. In Finland, the method has been used to treat various species of wood including aspen, birch, spruce, and pine. Wood species having poor properties can be treated using this method to alter the properties.[7] Similarly, the process has been adopted in France by Ecoles des Mines de Saint-Etienne using nitrogen as the drying gas. For the treatment at 210 °C, the material can be less brittle and the durability is improved. The cost of treatment was reported around 150−160 euro/m$^3$ treated wood.[12] Since the boiling point of oil is usually higher than the temperature of thermal treatment of wood using nitrogen atmosphere, thermal

**Received:** January 7, 2013
**Revised:** March 20, 2013
**Accepted:** April 3, 2013
**Published:** April 3, 2013





dx.doi.org/10.1021/ie4000689 | *Ind. Eng. Chem. Res.* 2013, 52, 6242−6252

treatment in oil bath has been implemented in Germany. This process has also been reported to improve the durability, smell, color, and surface properties of wood.[13]

For optimization and design of the heat treatment system, the effective mathematical model can be implemented. The model can assist in the development and construction of equipment, evaluate the performance of equipment, and assess the moisture content of wood resulting by the process. The mathematical model should ideally be able to capture major physics during process and require minimum number of experiments to generate the parameters. Several models have been proposed and implemented to model the high temperature treatment of wood.[1,14−16] The Whittaker approach was implemented by Younsi et al.[1] to model the heat treatment of wood with different final gas temperature and initial moisture content. Similarly, Luikov's approach was applied by Younsi et al.[14] to model the heat treatment of wood under different heating rate and final gas temperature. In addition, Kocaefe et al.[16] used diffusion-based model to model the heat treatment of wood. The models resulted in a reasonably good agreement toward experimental data but they tend to require many parameters to be generated.

Diffusion-based model is commonly used to describe the mass transfer process including drying and effective diffusivity is implemented in order to lump the whole phenomenon during drying (liquid diffusion, vapor diffusion, evaporation/condensation).[17−20] It has been analyzed that the effective diffusivity is actually interaction of several variables including moisture content, temperature, and pressure.[21,22] Application of the liquid diffusion only may not be able to represent the drying kinetics well because in the liquid diffusion equation, the evaporation is assumed to occur only at the surface of the materials being dried. For porous materials being dried, the evaporation should occur inside porous materials where the surface-solid water vapor concentration is higher than the concentration of water vapor inside the pore.[21−25] The liquid diffusion only also cannot yield the spatial profiles of water vapor concentration during drying. The profiles are important to obtain better understanding the transport phenomena of the drying process.[21,22]

For better understanding of transport phenomena of drying processes, a multiphase drying approach is suggested. The equilibrium and nonequilibrium drying approach can be implemented, but for more generic application, the nonequilibrium multiphase drying approach should be implemented; the model can be used to assess the applicability of the equilibrium multiphase drying approach.[22,23] The nonequilibrium multiphase drying approach is represented in a set of equations of conservation of mass in liquid and vapor phase as well as conservation of heat. The equations of conservation of mass in both phases are linked by internal evaporation/condensation rate.[21−23] An explicit and accurate formulation of the evaporation/condensation rate is necessary. Implementation of the rate derived from the moisture loss data was indicated to have lack of physical basis as it does not satisfy the mass balance. Unreasonable profiles of moisture content and/or temperature may result.[22] The rate should be affected by both moisture and vapor transport, and it can be related to the difference of equilibrium vapor pressure and the vapor pressure at particular time inside the pore.[22]

The reaction engineering approach (REA) was first suggested by X.D. Chen (the second author) in 1996 and has been implemented to model several challenging drying cases.[27−39] The REA was shown to be accurate and robust to model convective drying of thin layer or small food materials. For instance, modeling of the drying of an aqueous lactose solution droplet showed that the average absolute difference of weight loss profile was about 1% of the initial weight while that of temperature profile was only about 1.2 °C.[30] Application of REA to model drying of cream and whey protein concentrate showed average absolute difference of weight profile of 1.9% and 2.1%, respectively, while that of temperature was about 3 and 1.9 °C for cream and whey protein concentrate respectively.[31] The REA was also accurate to model drying of nonfood materials including the one with infrared-heating.[32] Application of the REA on the cyclic drying of polymer drying was indicated to be successful.[33] Application of the REA has also been extended not only on the thin layer or small food materials but also on the thick sample materials.[34,35] The combination of the REA and the approximation of the temperature distribution inside the sample can describe both moisture content and temperature profiles accurately.[34,35] The REA represented in its lumped format (i.e., ordinary differential equation with respect to time) is further called the lumped reaction engineering approach (L-REA). Recently, the L-REA has been applied to model the cyclic drying under time-varying humidity and temperature, the heat treatment of wood under time-varying gas temperature as well as the baking of thin layer of cake. The results of the modeling matched well with the experimental data. This indicates that the L-REA is indeed flexible to model the challenging drying cases.[36−39]

Although the nonequilibrium model is suggested as mentioned before, there has been no application of this model apart from the work of Kar and Chen[40,41] on drying of porcine skin. The S-REA has been applied to model convective drying of mango and potato tissues.[42] In S-REA, the REA was used to describe the local evaporation rate and combined with the mechanistic drying model. The results of modeling matched well with the experimental data.[42] The S-REA described the profiles of moisture content and temperature well. In addition, the S-REA yields advantages of generating the profiles of water vapor concentration during drying so that the better understanding of transport phenomena of drying process can be captured.[42]

In spite of the accuracy of the S-REA to model the convective drying of food materials under constant environmental conditions,[42] it may be challenging for the S-REA to model the heat treatment of wood since it involves time-varying gas temperature at relatively high temperature. This study is aimed to investigate and evaluate the applicability of the REA to model the local evaporation/condensation rate of simultaneous heat and mass transfer process involving water transformation under time-varying condition at relatively high temperature as well as investigate and evaluate the accuracy S-REA to model the heat treatment of wood under constant heating rate which is a relatively complex process to model. The outline of this subchapter is as follows: the experimental conditions are reviewed followed by the explanation of the S-REA modeling. Relevant discussions on the accuracy of the S-REA are provided subsequently.


dx.doi.org/10.1021/ie4000689 | Ind. Eng. Chem. Res. 2013, 52, 6242−6252

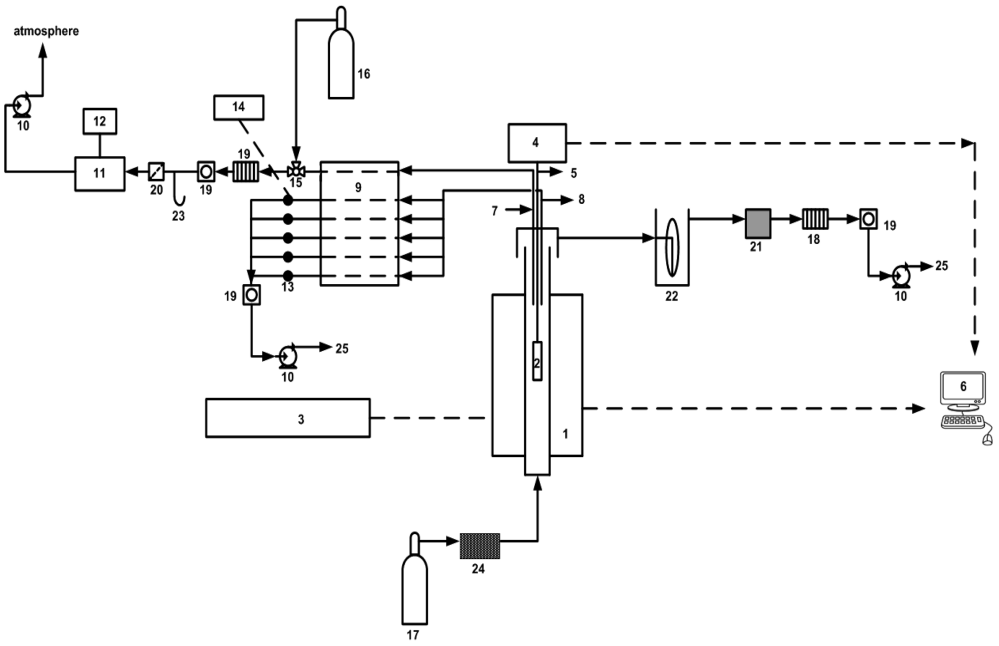


1. Furnace
2. Sample
3. Temperature controller
4. Balance
5. Hanger
6. Computer
7. Sampling probe for noncondensables
8. Sampling probe for condensables
9. Bubblers
10. Suction pump
11. Chromatograph
12. Integrator
13. Solanoid valves
14. Controller for solanoid valves
15. Three way valves
16. Calibration gas
17. Nitrogen
18. Resin filter
19. Flow meter
20. Paper filter
21. Glass wool
22. Cold trap
23. Manometer
24. Silica gel
25. Fume hood

**Figure 1.** Equipment setup of heat treatment of wood. Adapted with permission from ref 16. Copyright 2013 John Wiley and Sons.

## 2. REVIEW OF EXPERIMENTAL DETAILS AND THE SPATIAL REACTION ENGINEERING APPROACH (S-REA) TO MODEL THE HEAT TREATMENT OF WOOD UNDER CONSTANT HEATING RATE

The accuracy and robustness of the S-REA for heat treatment of wood under constant heating rate is benchmarked toward the experimental data of Younsi et al.[1,14,15] The experimental details were reported in the works of Kocaefe et al.[16,43] and Younsi et al.,[11] and these are reviewed here for better understanding of the current approach. A thermogravimetric analyzer was used for the heat treatment of wood as shown in Figure 1. Wood samples with dimensions of 0.035 × 0.035 × 0.2 m were heat treated by suspending the samples into a balance with accuracy of 0.001 g. The heat treatment was conducted by exposing the samples into hot gas whose temperature is linearly increased according to the heating rate. The humidity of gas is controlled by the injection of steam into the second furnace placed under the main furnace (refer to Figure 1). Initial moisture content of the samples was between 7 and 12 wt % (dry basis) and initial temperature of the samples was 20 °C (refer to Table 1). The samples were first heated to 120 °C and held at this temperature for half an hour followed by heating under the preset heating rate (refer to Table 1) until the final temperature (also refer to Table 1) is achieved.

The adaptation of the L-REA described previously[23,27−39] to spatially distributed cases (i.e., S-REA) to model the heat treatment of wood is described here. In experiments reported previously[14,15] which is the subject of interest, 2D modeling with respect to $x$ and $y$ directions can be setup as the height of the sample (0.2 m) is much higher than the length (0.035 m) and width (0.035m) of the sample. The mass balance of water in the liquid phase is written as[22,26,42,44]

**Table 1. Experimental Settings of Heat Treatment of Wood[14,15]**

| case | final gas temperature (°C) | heating rate (°C $h^{-1}$) | initial moisture content (kg $H_2O$ kg dry solids$^{-1}$) |
|---|---|---|---|
| 1 | 220 | 10 | 0.11 |
| 2 | 220 | 20 | 0.125 |
| 3 | 220 | 30 | 0.12 |
| 4 | 200 | 20 | 0.07 |

$$\frac{\partial(C_s X)}{\partial t} = \frac{\partial}{\partial x}\left(D_w \frac{\partial(C_s X)}{\partial x}\right) + \frac{\partial}{\partial y}\left(D_w \frac{\partial(C_s X)}{\partial y}\right) - \dot{I} \quad (1)$$

Meanwhile, the mass balance of water in the vapor phase is expressed as[22,26,42,44]

$$\frac{\partial C_v}{\partial t} = \frac{\partial}{\partial x}\left(D_v \frac{\partial C_v}{\partial x}\right) + \frac{\partial}{\partial y}\left(D_v \frac{\partial C_v}{\partial y}\right) + \dot{I} \quad (2)$$

The heat balance is represented as[22,26,42,44]

$$\rho C_p \frac{\partial T}{\partial t} = \frac{\partial}{\partial x}\left(k \frac{\partial T}{\partial x}\right) + \frac{\partial}{\partial y}\left(k \frac{\partial T}{\partial y}\right) - \dot{I}\Delta H_v \quad (3)$$


dx.doi.org/10.1021/ie4000689 | Ind. Eng. Chem. Res. 2013, 52, 6242−6252

The initial and boundary conditions for eqs 1−3 are

$$t = 0, \quad X = X_o, \quad C_v = C_{vo}, \quad T = T_o \tag{4}$$

$$x = 0, \quad y = 0, \quad \frac{dX}{dx} = 0, \quad \frac{dC_v}{dx} = 0, \quad \frac{dT}{dx} = 0, \quad \frac{dX}{dy} = 0, \quad \frac{dC_v}{dy} = 0, \quad \frac{dT}{dy} = 0 \tag{5}$$

$$x = L, \quad y = L, \quad -C_s D_w \frac{dX}{dx} = h_m \varepsilon_w \left( \frac{C_{v,s}}{\varepsilon} - \rho_{v,b} \right), \quad -C_s D_w \frac{dX}{dy} = h_m \varepsilon_w \left( \frac{C_{v,s}}{\varepsilon} - \rho_{v,b} \right) \tag{6}$$

$$-D_v \frac{dC_v}{dx} = h_m \varepsilon_v \left( \frac{C_{v,s}}{\varepsilon} - \rho_{v,b} \right), \quad -D_v \frac{dC_v}{dy} = h_m \varepsilon_v \left( \frac{C_{v,s}}{\varepsilon} - \rho_{v,b} \right) \tag{7}$$

$$k \frac{dT}{dx} = h(T_b - T), \quad k \frac{dT}{dy} = h(T_b - T) \tag{8}$$

Because the sample was dried uniformly from all directions and the dimension of length and width is the same, the mass balance of water in liquid phase can be simplified into[42,45,46]

$$\frac{\partial (C_s X)}{\partial t} = 2 \frac{\partial}{\partial x} \left( D_w \frac{\partial (C_s X)}{\partial x} \right) - \dot{I} \tag{9}$$

while the mass balance of water in vapor phase can be expressed as[42,45,46]

$$\frac{\partial C_v}{\partial t} = 2 \frac{\partial}{\partial x} \left( D_v \frac{\partial C_v}{\partial x} \right) + \dot{I} \tag{10}$$

In addition, the heat balance can be represented as[42,45,46]

$$\rho C_p \frac{\partial T}{\partial t} = 2 \frac{\partial}{\partial x} \left( k \frac{\partial T}{\partial x} \right) - \dot{I} \Delta H_v \tag{11}$$

$\dot{I}$ is the local drying rate within the solid structure described as[42,45,46]

$$\dot{I} = h_{m_{in}} A_{in} (C_{v,s} - C_v) \tag{12}$$

By implementing the REA, internal-surface water vapor concentration can be written as[40−42]

$$C_{v,s} = \exp \left( \frac{-\Delta E_v}{RT} \right) C_{v,sat} \tag{13}$$

Therefore, the local drying or wetting rate can be expressed as[40−42]

$$\dot{I} = h_{m_{in}} A_{in} \left( \exp \left( \frac{-\Delta E_v}{RT} \right) C_{v,sat} - C_v \right) \tag{14}$$

The relative activation energy of heat treatment of wood is generated from experiment of heat treatment of wood of case 2 (refer to Table 1).[15] The procedures to evaluate activation energy, equilibrium activation energy and relative activation energy have been explained previously.[27−39] The relationship between the relative activation energy and average moisture content can be represented by a simple mathematical equation obtained by the least-squares method using Microsoft Excel.[47] The relative activation energy can be represented as

$$\frac{\Delta E_v}{\Delta E_{v,b}} = [1 - 1.517(\bar{X} - X_b)^{0.22}] \exp[-3.717(\bar{X} - X_b)^{3.135}] \tag{15}$$

The good agreement between the fitted and experimental relative activation energy is shown by $R^2$ of 0.98. For modeling using the S-REA here, the relative activation energy shown in eq 15 is used but the average moisture content $\bar{X}$ in eq 15 is substituted by the local moisture content ($X$). The effective vapor diffusivity is deduced from[48]

$$D_v = D_{vo} \frac{\varepsilon}{\tau} \tag{16}$$

The water vapor diffusivity ($m^2 \cdot s^{-1}$) can be expressed as[49]

$$D_{vo} = 2.09 \times 10^{-5} + 2.137 \times 10^{-7} (T - 273.15) \tag{17}$$

The turtuosity ($\tau$) can be represented as[50,51]

$$\tau = \varepsilon^{-n} \tag{18}$$

$n = 0.5$ is chosen in this study. $C_s$ is the solid concentration which can be deduced by[40−42]

$$C_s = \frac{1 - \varepsilon}{\frac{1}{\rho_s} + \frac{X}{\rho_w}} \tag{19}$$

The porosity ($\varepsilon$), dependent on the local moisture content, can be determined by[52]

$$\varepsilon = 1 - \frac{V_0}{V} (1 - \varepsilon_0) \left( \frac{\frac{\rho_s}{\rho_w} \bar{X} + 1}{1 + \frac{\rho_s}{\rho_w} X_0} \right) \tag{20}$$

Initially, the moisture is present in the void spaces of pores and within the pores. As drying proceeds, the moisture may migrate within the pores by liquid diffusion and thereafter from the surface of the pores by vapor diffusion. Even at low water content, "surface" diffusion could occur along the pore surface accessible to air.[53] The internal mass transfer coefficient shown in eq 12 incorporates the restriction factor as it may be affected by the pore structure and pore network inside the samples. This makes the value of $h_{m,in}$ grow from small value to the value of $D_v/r_p$ (when $\Theta = 1$).[40,41,54] In this study, $h_{m,in}$ of 0.001 $m \cdot s^{-1}$ is chosen as it is in the order of $D_v/r_p$ (hence deterministic). The effective liquid water diffusivity ($D_w$) is determined from the experiments of heat treatment of wood in order to match the results of modeling with the experimental data. So far, no method has been presented anywhere in the literatures to measure the "pure liquid diffusivity".

For modeling the heat treatment of wood under constant heating rate which is essentially a drying process under linearly increased gas temperature, the equilibrium activation energy shown is evaluated according to corresponding gas temperature and humidity during the process. The equilibrium activation energy is then combined with the relative activation energy shown in eq 15. In addition, the boundary condition of heat balance shown in eq 8 implements the linearly increased gas temperature. In order to yield the spatial profiles during the heat treatment of wood, eqs 9−11 in conjunction with the initial and boundary conditions represented in eqs 4−8 as well as the equilibrium and relative activation energy are solved by


dx.doi.org/10.1021/ie4000689 | Ind. Eng. Chem. Res. 2013, 52, 6242−6252

method of lines.[55,56] The ordinary differential equations are then solved simultaneously by *ode23s* in Matlab. The spatial derivative here is discretized into ten increments; application of 100 increments has been conducted and there is no difference in the profiles observed as shown in Figure 2. No shrinkage is incorporated in the modeling as Younsi et al.[14] indicated that the ratio between the final and initial dimension is around 0.96.

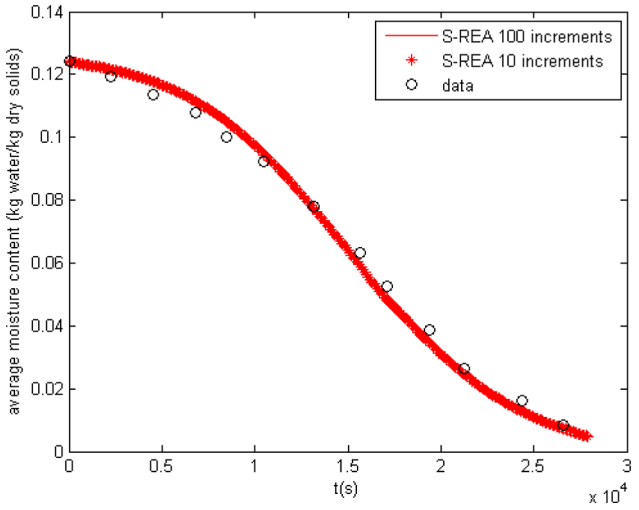


**Figure 2.** Profiles of average moisture content during heat treatment of case 2 (refer to Table 1) solved using method of lines using 10 and 100 increments.

## 3. RESULTS AND DISCUSSION

The S-REA is used here to model the heat treatment of wood under constant heating rate and the results of modeling are presented in Figures 3−15. The REA is implemented to model

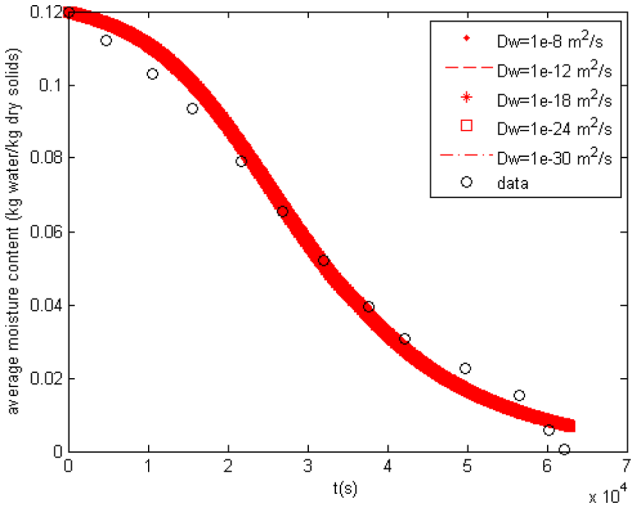


**Figure 3.** Effect of liquid diffusivity on profiles of moisture content of heat treatment of case 1 (refer to Table 1).

the local evaporation or condensation term and coupled with a system of equations in order to yield the spatial profiles of moisture content, water vapor concentration, and temperature. It is noted that if locally there is no vacant pore space which is connected with other pores or channels, the internal mass transfer area is zero, hence the REA term is zero. In this study, the internal mass transfer coefficient ($h_{m,in}$) shown in eq 12 is chosen to be 0.001 m·s$^{-1}$. Application of $h_{m,in}$ higher than 0.001 m·s$^{-1}$ does not yield any noticeable differences in the profiles of moisture content and temperature profiles. More importantly, the $h_{m,in}$ of 0.001 m·s$^{-1}$ is on the order of $D_v/r_p$, as suggested by Kar and Chen.[40,41]

As mentioned before, no method has been presented anywhere in the literatures to measure the pore liquid diffusivity and the liquid diffusivity is obtained by the numerical sensitivity to match the predicted with the experimental data of moisture content and temperature. Interestingly, in this study, for all cases the profiles of moisture content and temperature is independent of the value of liquid diffusivity. Further explanation about this phenomenon is presented below.

For case 1 (refer to Table 1), the results of modeling are presented in Figures 3−6. For case 1, the varied values of the liquid diffusivity in the range of $1 \times 10^{-8}$ to $1 \times 10^{-30}$ m$^2$·s$^{-1}$ have been used and there are no noticeable differences in the profiles of moisture content and temperature as shown in Figures 3 and 4. This may indicate that the modeling of heat

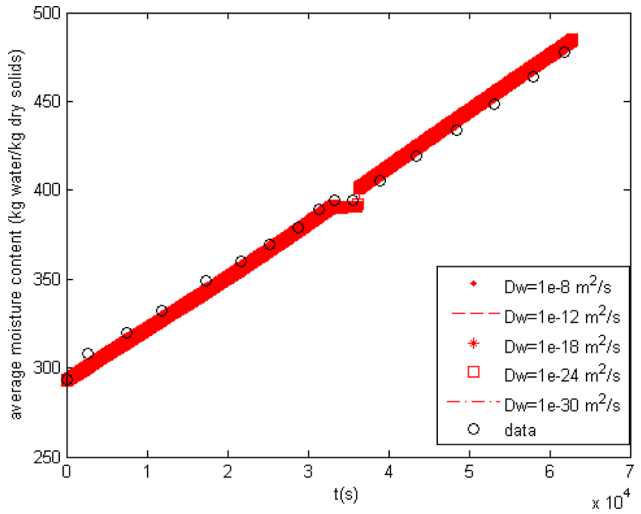


**Figure 4.** Effect of liquid diffusivity on profiles of temperature of heat treatment of case 1 (refer to Table 1).

treatment of case 1 is independent of the value of liquid diffusivity. The phenomenon could be because the initial moisture content is relatively low and the heat treatment of wood implemented relatively high temperature. Without using the liquid diffusion term on the mass balance of liquid water (refer to eq 9), a good agreement between the predicted and experimental data of moisture content and temperature is shown in Figures 5 and 6 as well as confirmed by $R^2$ and RMSE indicated in Table 2. Benchmarks against modeling implemented by Younsi et al.[15] indicate that the S-REA yields comparable or even better results. Therefore, it can be said that the S-REA model the heat treatment of wood of case 1 (refer to Table 1) well.

Figures 7−11 show the results of modeling of heat treatment of wood of case 2 (refer to Table 1). Similar to case 1, the varied values of the liquid diffusivity in the range of $1 \times 10^{-8}$ to $1 \times 10^{-30}$ m$^2$·s$^{-1}$ have been used and there is no noticeable effect on the profiles of moisture content and temperature. Without using the liquid diffusion term in the mass balance of liquid water (refer to eq 9), a good agreement between the predicted and experimental data of moisture content and


dx.doi.org/10.1021/ie4000689 | Ind. Eng. Chem. Res. 2013, 52, 6242−6252

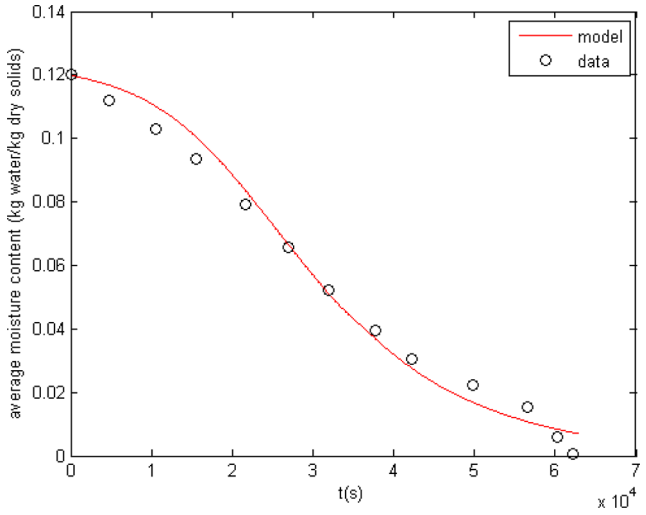


**Figure 5.** Profiles of average moisture content during heat treatment of case 1 (refer to Table 1).

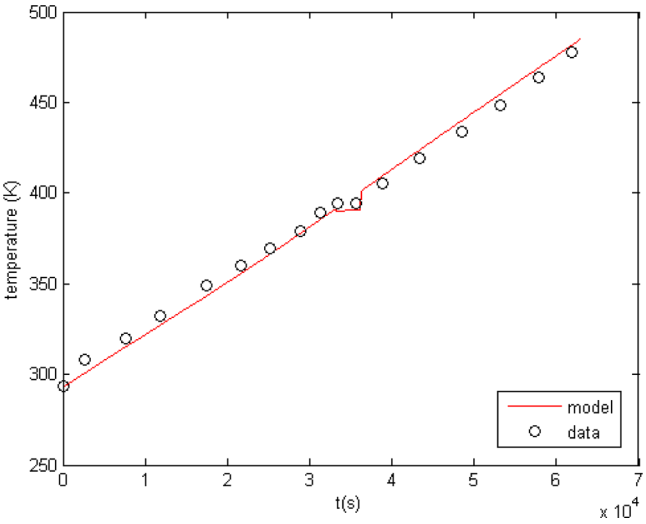


**Figure 6.** Profiles of temperature during heat treatment of case 1 (refer to Table 1).

**Table 2. $R^2$ and RMSE of Modeling of Heat Treatment of Wood under Constant Heating Rate Using S-REA**

| case | $R^2$ for $X$ | $R^2$ for $T$ | RMSE for $X$ | RMSE for $T$ |
|---|---|---|---|---|
| 1 | 0.988 | 0.992 | 0.004 | 4.765 |
| 2 | 0.995 | 0.997 | 0.003 | 3.287 |
| 3 | 0.987 | 0.995 | 0.004 | 3.756 |
| 4 | 0.99 | 0.998 | 0.002 | 2.617 |

temperature is shown in Figures 7 and 8 and confirmed by $R^2$ and RMSE as shown in Table 2. The S-REA describes the profiles of moisture content and temperature very well. Benchmarks against modeling implemented by Younsi et al.[15] reveal that the S-REA yields better agreement toward the experimental data of moisture content.

The spatial profiles of moisture content, water vapor concentration, and temperature are presented in Figures 9–11. Figure 9 indicates that the moisture content of the inner part of the samples is higher than that of the outer part which indicates the moisture migrates outward during drying. Similarly, as shown in Figure 10, the water vapor concentration

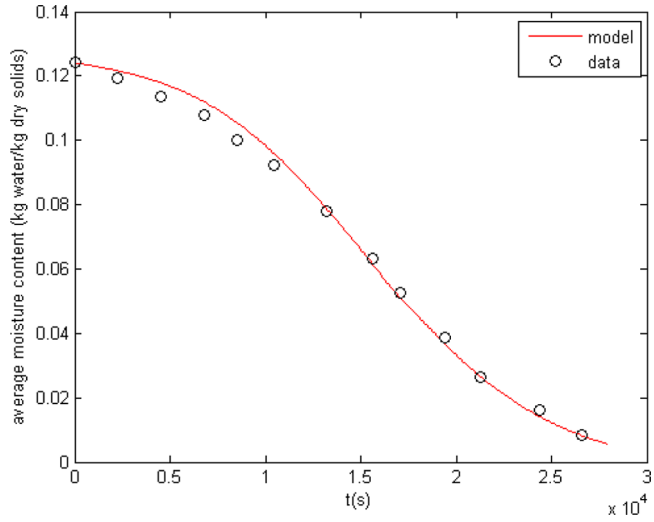


**Figure 7.** Profiles of average moisture content during heat treatment of case 2 (refer to Table 1).

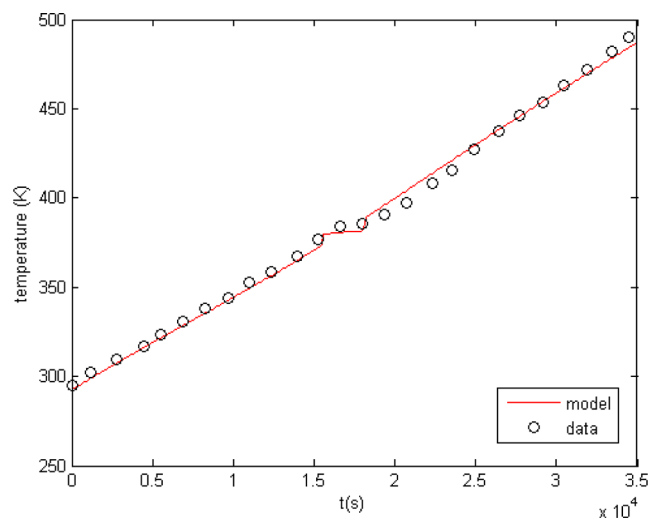


**Figure 8.** Profiles of temperature during heat treatment of case 2 (refer to Table 1).

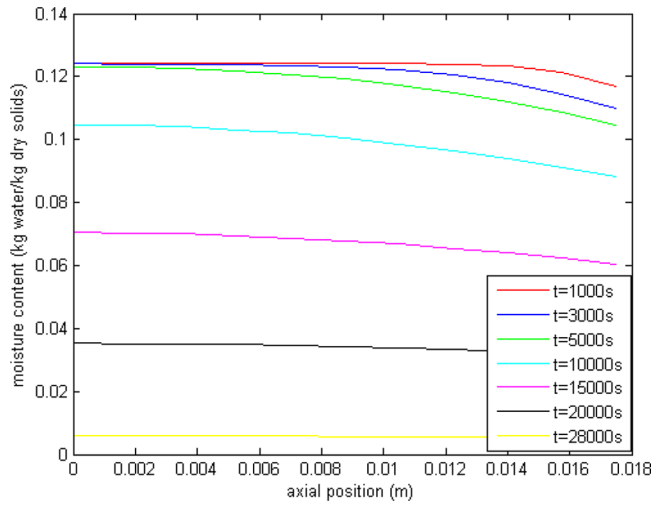


**Figure 9.** Profiles of spatial moisture content during heat treatment of case 2 (refer to Table 1).


dx.doi.org/10.1021/ie4000689 | Ind. Eng. Chem. Res. 2013, 52, 6242–6252

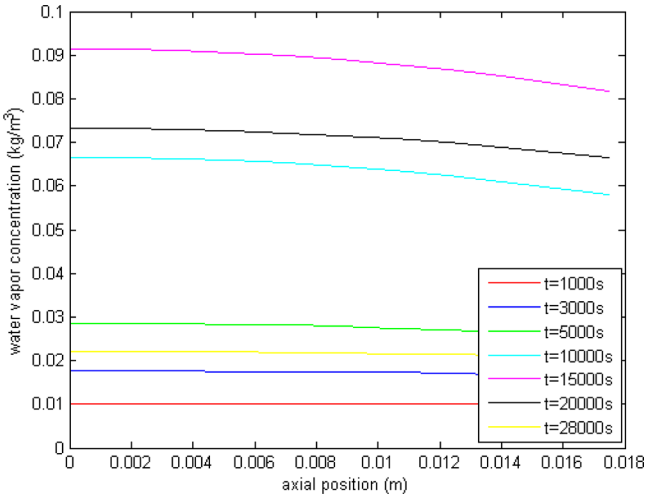


**Figure 10.** Profiles of spatial water vapor concentration during heat treatment of case 2 (refer to Table 1).

of the inner part of the samples is higher than that of the outer part. This could be because of the relatively high initial porosity of the samples which allows the evaporation at the core of the samples. The water vapor seems to migrate outward, and at the surface, it is taken away by the gas. The water vapor concentration increases until heating time of 15 500 s followed by a decrease until the end of drying. The initial increase could be because the initial moisture content is still relatively high at the beginning of drying but as the heating progresses, the moisture content decreases and lower water vapor is generated. As shown in Figure 11, the temperature distribution of the samples is essentially uniform, in agreement with the observation of Younsi et al.[14]

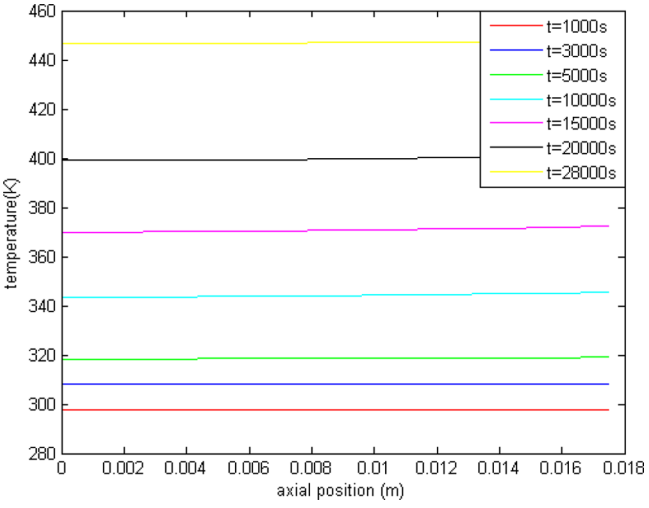


**Figure 11.** Profiles of spatial temperature during heat treatment of case 2 (refer to Table 1).

For case 3 (refer to Table 1), the results of modeling are presented in Figures 12 and 13. Again, the varied values of liquid diffusivity do not give any noticeable differences in the profiles of moisture content and temperature. Similar to cases 1 and 2, without using the liquid diffusion term in the mass balance of liquid water (refer to eq 9), the results of modeling match well with the experimental data as indicated in Figures 12 and 13 as well as confirmed by $R^2$ and RMSE shown in

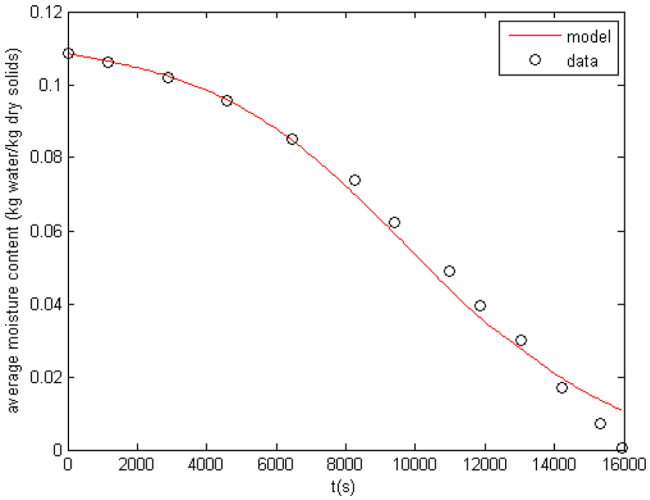


**Figure 12.** Profiles of average moisture content during heat treatment of case 3 (refer to Table 1).

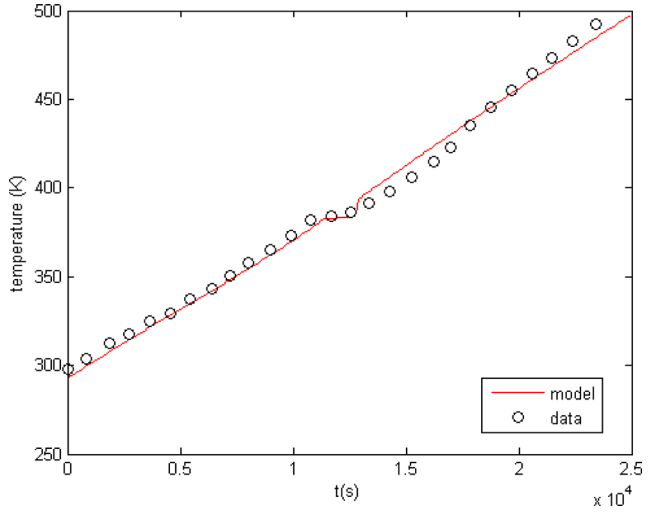


**Figure 13.** Profiles of temperature during heat treatment of case 3 (refer to Table 1).

Table 2. Benchmarks against modeling used by Younsi et al.[15] indicate that the S-REA results in a better agreement toward the experimental data. The S-REA models the heat treatment of wood of case 3 (refer to Table 1) well.

Figures 14 and 15 show the results of modeling of case 4 (refer to Table 1). Again, without using the liquid diffusion term, a good agreement between the predicted and experimental data is observed and confirmed by $R^2$ and RMSE shown in Table 2. Benchmarks against modeling implemented by Younsi et al.[14] show that the S-REA performs better. It can be said that the S-REA is accurate to model the heat treatment of wood of case 4 (refer to Table 1).

It can be observed that for all cases investigated, the S-REA can model the heat treatment of wood under constant heating rate very well. It seems that the model does not need the liquid diffusion term. This could be due to the relatively low initial moisture content of the samples and the process implemented at relatively high temperature. The profiles of water vapor concentration during the process can also be generated by the S-REA so that better understanding of the transport phenomena of the process can be obtained. It can be said here that the REA can model well the local evaporation/


dx.doi.org/10.1021/ie4000689 | Ind. Eng. Chem. Res. 2013, 52, 6242−6252

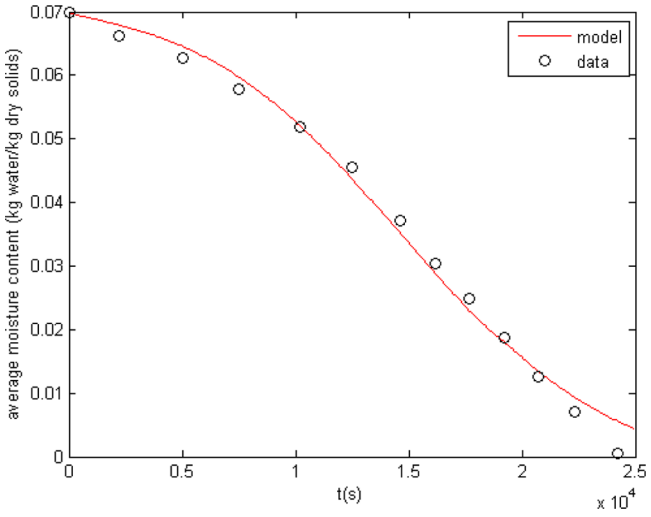


**Figure 14.** Profiles of average moisture content during heat treatment of case 4 (refer to Table 1).

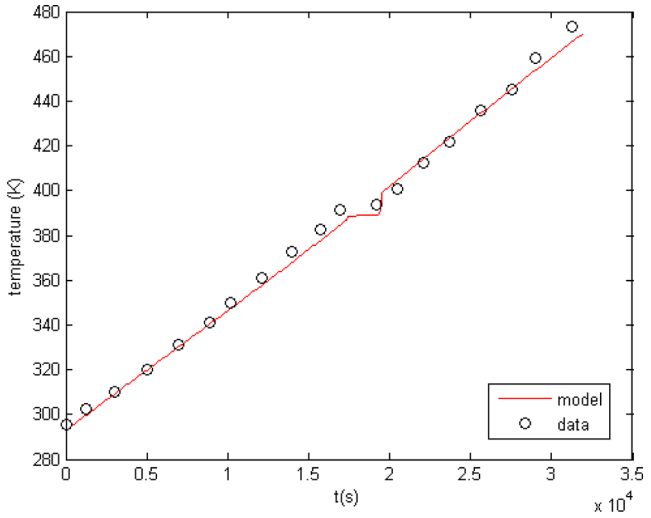


**Figure 15.** Profiles of temperature during heat treatment of case 4 (refer to Table 1).

condensation rate of the heat treatment of wood under constant heating rate. The S-REA is an effective multiphase approach to model the heat treatment of wood which is essentially a simultaneous heat and mass transfer process involving water transformation under time-varying conditions at relatively high temperature.

Both L-REA (lumped reaction engineering approach) and S-REA (spatial reaction engineering approach) are capable for modeling several challenging drying cases.[32−39] However, the L-REA is presented in lumped format (ordinary differential equation with respect to time), the L-REA only project the average moisture content during drying. The L-REA can actually model drying of materials with thickness of several centimeters which have a *Chen_Biot* number (*Ch_Bi*) of 0.3.[34,35] For modeling drying of even thicker materials, the prediction of spatial profiles of temperature inside the samples are necessary. Hence, the S-REA becomes necessary.

On the basis of the case studies 1−4 above, it appears that the S-REA can be used to model the heat treatment well. The S-REA may be adopted in industry implementing thermal treatment of wood such as Thermowood Technology.[7] As mentioned before, Thermowood Technology[7] modifies the properties of wood and increases its quality by exposing wood into linearly increased gas temperature in various steps. The S-REA may be used to explore the various scenarios of heat treatment on the wood properties and assess the wood properties resulted. The S-REA can predict the profiles of moisture content, spatial water vapor concentration, and temperature inside the wood samples. These variables may then be used to estimate the wood properties. Because the S-REA yields the spatial profiles of the variables, the spatial profiles of wood properties can be studied. For exploration of the heat treatment of new wood samples, the REA framework is very useful since the S-REA only requires one set of accurate run to establish the REA parameters.

The S-REA can also be used to assist in process design of new equipment and analysis of energy efficiency. The S-REA can be coupled with computational fluid dynamics (CFD) based simulations to predict the flow-field of the drying air so that the profiles of velocity, water vapor concentration, and temperature of the drying air can be studied. Due to the accuracy of the REA framework, the energy consumption can be evaluated. Several scenarios for minimization of energy consumption can be studied by simulations using the REA framework.

## 4. CONCLUSION

In this study, the S-REA is implemented to model the heat treatment of wood under constant heating rate. The REA is used to describe the local evaporation/condensation rate and combined with a system of equations of conservation to yield the spatial profiles of moisture content, water vapor concentration, and temperature. The results of modeling match well with the experimental data. The S-REA describes the profiles of moisture content, concentration of water vapor, and temperature well. The REA is applicable to model the local evaporation rate of the simultaneous heat and mass transfer process involving water transformation under time-varying conditions at relatively high temperature. The S-REA is an effective nonequilibrium multiphase approach to model the simultaneous heat and mass transfer process under time-varying conditions at relatively high temperature.

## APPENDIX A: DETERMINATION OF HEAT AND MASS TRANSFER COEFFICIENT AND PHYSICAL PROPERTIES OF WOOD SAMPLES[45,57,58]

Heat and mass transfer coefficients are determined by

$$Nu = 0.664Re^{0.5}Pr^{0.333} \tag{A1}$$

$$Sh = 0.664Re^{0.5}Sc^{0.333} \tag{A2}$$

where *Nu* is the Nusselt number, *Re* is the Reynolds number, *Pr* is the Prandtl number, and *Sc* is the Schmidt number.

$$\rho = 660(1 + 0.01M) \tag{A3}$$

where $\rho$ is the density of wood samples ($kg \cdot m^{-3}$), $M$ is the moisture content on dry basis (kg $H_2O$·kg dry basis$^{-1}$)

$$C_p = \frac{C_{po} + 0.01C_{pw}}{1 + 0.01M} + A_c \tag{A4}$$

where $C_p$ is the specific heat of the wood samples ($kJ \cdot kg \cdot K^{-1}$), $C_{po}$ is the specific heat of the dry wood ($kJ \cdot kg \cdot K^{-1}$), $C_{pw}$ is the


dx.doi.org/10.1021/ie4000689 | Ind. Eng. Chem. Res. 2013, 52, 6242−6252

specific heat of water (kJ·kg·K$^{-1}$), and $A_c$ is the parameters as function of moisture content and temperature

$$C_{po} = 0.1031 + 0.003867T \quad \text{(A5)}$$

where $T$ is the temperature (K)

$$C_{pw} = -2 \times 10^{-12}T^5 + 4.39 \times 10^{-9}T^4 - 3.56 \times 10^{-6}T^3 + 1.4327 \times 10^{-3}T^2 - 285.6 \times 10^{-3}T + 26.779 \quad \text{(A6)}$$

$$A_c = M(-0.06191 + 2.36 \times 10^{-4}T - 1.33 \times 10^{-4}M) \quad \text{(A7)}$$

## APPENDIX B: EVALUATION OF INTERNAL SURFACE AREA ($A_{IN}$)[40,41,54]

$$A_p = 4\pi r_p^2 \quad \text{(B1)}$$

$$V_p = \frac{4}{3}\pi r_p^3 \quad \text{(B2)}$$

$$m_p = \rho_p V_p(1 - v_w) \quad \text{(B3)}$$

$$N = \frac{m_s}{m_p} \quad \text{(B4)}$$

$$n_p = \frac{N}{V_s} \quad \text{(B5)}$$

$$A_{in} = n_p A_p \quad \text{(B6)}$$

## AUTHOR INFORMATION


### Corresponding Author

*Corresponding author's e-mail: dong.chen@monash.edu; xdc@xmu.edu.cn; xdchen@suda.edu.cn.


### Notes

The authors declare no competing financial interest.

## NOMENCLATURES

$A$ = surface area of samples (m$^2$)
$A_{in}$ = internal surface area per unit volume (m$^2$·m$^{-3}$)
$A_o$ = initial surface area of samples (m$^2$)
$A_p$ = cell surface area (m$^2$)
$C_p$ = specific heat of sample (J·kg·K$^{-1}$)
$C_{ps}$ = specific heat of solids (J·kg$^{-1}$·K$^{-1}$)
$C_{pw}$ = specific heat of water (J·kg$^{-1}$·K$^{-1}$)
$C_s$ = solid concentration (kg·m$^{-3}$)
$C_v$ = water vapor concentration (kg·m$^{-3}$)
$C_{v,s}$ = internal-surface vapor concentration (kg·m$^{-3}$)
$C_{v,sat}$ = internal-saturated vapor concentration (kg·m$^{-3}$)
$D_v$ = effective water vapor diffusivity (m·s$^{-2}$)
$D_{v,o}$ = water vapor diffusivity (m·s$^{-2}$)
$D_w$ = capillary diffusivity (m·s$^{-2}$)
$h$ = heat transfer coefficient (W·m$^{-2}$·K$^{-1}$)
$h_m$ = mass transfer coefficient (m·s$^{-1}$)
$h_{m,in}$ = internal mass transfer coefficient (m·s$^{-1}$)
$I$ = local evaporation rate (kg·m$^{-3}$·s$^{-1}$)
$k$ = thermal conductivity of sample (W·m$^{-1}$·K$^{-1}$)
$m_p$ = dry mass of cell (kg)
$m_s$ = dried mass sample of material (kg)
$n$ = constant
$N$ = number of cell in samples
$n_p$ = number of cell per unit volume (m$^{-3}$)
$r$ = radial position (m)
$RH_b$ = relative humidity of gas
$r_p$ = cell radius (m)
$T$ = sample temperature (K)
$T_s$ = surface sample temperature (K)
$t$ = time (s)
$T_b$ = gas temperature (K)
$V_p$ = cell volume (m$^3$)
$w$ = mass fraction of water
$X$ = moisture content on dry basis (kg·kg$^{-1}$)
$\bar{X}$ = average moisture content on dry basis (kg·kg$^{-1}$)
$X_b$ = equilibrium moisture content on dry basis (kg·kg$^{-1}$)
$X_o$ = initial moisture content (kg·kg$^{-1}$)
$\Delta E_v$ = apparent activation energy (J·mol$^{-1}$)
$\Delta E_{v,b}$ = "equilibrium" activation energy (J·mol$^{-1}$)
$\Delta H_v$ = vaporization heat of water (J·kg$^{-1}$)
$\varepsilon$ = porosity
$\varepsilon_w$ = fraction by liquid water
$\varepsilon_v$ = fraction by water vapor
$\varepsilon_o$ = initial porosity
$\Theta$ = constriction factor
$\rho$ = sample density (kg·m$^{-3}$)
$\rho_s$ = density of solids (kg·m$^{-3}$)
$\rho_{v,b}$ = vapor concentration in drying medium (kg·m$^{-3}$)
$\rho_{v,s}$ = surface vapor concentration (kg·m$^{-3}$)
$\rho_{v,sat}$ = saturated vapor concentration (kg·m$^{-3}$)
$\rho_w$ = density of water (kg·m$^{-3}$)
$\tau$ = turtuosity

## REFERENCES


(1) Younsi, R.; Kocaefe, D.; Poncsak, S.; Kocaefe, Y. Transient multiphase model for the high-temperature thermal treatment of wood. *AIChE J.* **2006**, *52*, 2340−2349.

(2) Helsen, L.; Bulck, E. V. D. Review of disposal technologies for chromated copper arsenate (CCA) treated wood waste, with detailed analyses of thermochemical conversion processes. *Environ. Pollut.* **2005**, *134*, 301−314.

(3) Esteves, B.; Pereira, H. Wood modification by heat treatment: a review. *Bioresource* **2009**, *4*, 370−404.

(4) Gunduz, G.; Aydemir, D.; Karakas, G. The effects of thermal treatment on the mechanical properties of wild pear (*Pyrus elaegnifolia* Pall.) wood and changes in physical properties. *Mater. Des.* **2009**, *30*, 4391−4395.

(5) Mitchell, P. H. Irreversible property changes of small loblolly pine specimens heated in air, nitrogen, or oxygen. *Wood Fiber Science* **1988**, *20*, 320−355.

(6) Yildiz, S. *Physical, mechanical, technological and chemical properties of beech and spruce wood treated by heating*. PhD dissertation. Karadeniz Technical University, Trabzon, 2002.

(7) Thermowood Inc. www.thermowood.fi (accessed Dec 2012).

(8) Brosse, N.; El Hage, R.; Chaouch, M.; Petrissans, M.; Dumarçay, S.; Gerardin, P. Investigation of the chemical modifications of beech wood lignin during heat treatment. *Polym. Degrad. Stab.* **2010**, *95*, 1721−1726.

(9) Brito, J. O.; Silva, F. G.; Leao, M. M.; Almeida, G. Chemical composition changes in eucalyptus and pinus woods submitted to heat treatment. *Bioresour. Technol.* **2008**, *99*, 8545−8548.

(10) Hakkou, M.; Petrissans, M.; Zoulalian, A.; Gerardin, P. Investigation of wood wettability changes during heat treatment on the basis of chemical analysis. *Polym. Degrad. Stab.* **2005**, *89*, 1−5.

(11) Gonzalez-Pena, M. M.; Curling, S. F.; Hale, M. D. C. On the effect of heat on the chemical composition and dimensions of thermally-modified wood. *Polym. Degrad. Stab.* **2009**, *94*, 2184−2193.

(12) Vernois, M. Heat treatment of wood in France-state of the art. Review on heat treatments of wood. In *Proceedings of the special seminar held in Antibes, France*, Feb 9, 2001.
(13) Rapp, A. O.; Sailer, M. Oil heat treatment in Germany- state of the art. Review of heat treatment of wood. In *Proceedings of the special seminar held in Antibes, France*, Feb 9, 2001.
(14) Younsi, R.; Kocaefe, D.; Poncsak, S.; Kocaefe, Y. Thermal modelling of the high temperature treatment of wood based on Luikov's approach. *Int. J. Energy Res.* **2006**, *30*, 699−711.
(15) Younsi, R.; Kocaefe, D.; Poncsak, S.; Kocaefe, Y. Computational modelling of heat and mass transfer during the high-temperature heat treatment of wood. *Appl. Thermal Eng.* **2007**, *27*, 1424−1431.
(16) Kocaefe, D.; Charette, A.; Ferland, J.; Couderc, P.; Saint-Romain, J. L. A kinetic study of pyrolysis in pitch impregnated electrodes. *Can. J. Chem. Eng.* **1990**, *68*, 988−996.
(17) Nguyen, T. A.; Verboven, P.; Scheerlinck, N.; Vandewalle, S.; Nicolai, B. M. Estimation of effective diffusivity of pear tissue and cuticle by means of a numerical water diffusion model. *J. Food Eng.* **2006**, *72*, 63−72.
(18) Batista, L. M.; da Rosa, C. A.; Pinto, L. A. A. Diffusive model with variable effective diffusivity considering shrinkage in thin layer drying of chitosan. *J. Food Eng.* **2007**, *81*, 127−132.
(19) Corzo, O.; Bracho, N.; Alvarez, C. Water effective diffusion coefficient of mango slices at different maturity stages during air drying. *J. Food Eng.* **2008**, *87*, 479−484.
(20) Roberts, J. S.; Kidd, D. R.; Padilla-Zakour, O. Drying kinetics of grape seeds. *J. Food Eng.* **2008**, *89*, 460−465.
(21) Chen, X. D. Moisture diffusivity in food and biological materials. *Drying Tech.* **2007**, *25*, 1203−1213.
(22) Zhang, J.; Datta, A. K. Some considerations in modeling of moisture transport in heating of hygroscopic materials. *Drying Tech.* **2004**, *22*, 1983−2008.
(23) Chen, X. D.; Xie, G. Z. Fingerprints of the drying behavior of particulate or thin layer food materials established using a reaction engineering model. *Trans Inst. Chem. Eng., Part C: Food Bioprod. Proc.* **1997**, *75*, 213−222.
(24) Bazer-Bachi, F.; Augier, F.; Santos, B. 1D and 2D simulations of partially wetted catalyst particles: A focus on heat transfer limitations. *Chem. Eng. Sci.* **2011**, *66*, 1953−1961.
(25) Ousegui, A.; Moresoli, C.; Dostie, M.; Marcos, B. Porous multiphase approach for baking process − Explicit formulation of evaporation rate. *J. Food Eng.* **2010**, *100*, 535−544.
(26) Datta, A. K. Porous media approaches to studying simultaneous heat and mass transfer in food processes. I: Problem formulations. *J. Food Eng.* **2007**, *80*, 80−95.
(27) Chen, X. D.; Pirini, W.; Ozilgen, M. The reaction engineering approach to modeling drying of thin layer pulped kiwifruit flesh under conditions of small Biot numbers. *Chem. Eng. Proc.* **2001**, *40*, 311−320.
(28) Chen, X. D.; Lin, S. X. Q. Air drying of milk droplet under constant and time dependent conditions. *AIChE J.* **2005**, *51*, 1790−1799.
(29) Lin, S. X. Q.; Chen, X. D. Prediction of air drying of milk droplet under relatively high humidity using the reaction engineering approach. *Drying Tech.* **2005**, *23*, 1396−1406.
(30) Lin, S. X. Q.; Chen, X. D. A model for drying of an aqueous lactose droplet using the reaction engineering approach. *Drying Tech.* **2006**, *24*, 1329−1334.
(31) Lin, S. X. Q.; Chen, X. D. The reaction engineering approach to modeling the cream and whey protein concentrate droplet drying. *Chem. Eng. Proc.* **2007**, *46*, 437−443.
(32) Putranto, A.; Chen, X. D.; Webley, P. A. Infrared and convective drying of thin layer of polyvinyl alcohol (PVA)/glycerol/water mixture - The reaction engineering approach (REA). *Chem. Eng. Proc.: Process Intens.* **2010**, *49*, 348−357.
(33) Putranto, A.; Chen, X. D.; Webley, P. A. Application of the reaction engineering approach (REA) to model cyclic drying of polyvinyl alcohol(PVA)/glycerol/water mixture. *Chem. Eng. Sci.* **2010**, *65*, 5193−5203.
(34) Putranto, A.; Chen, X. D.; Webley, P. A. Modeling of drying of thick samples of mango and apple tissues using the reaction engineering approach (REA). *Drying Tech.* **2011**, *29*, 961−973.
(35) Putranto, A.; Chen, X. D.; Xiao, Z.; Webley, P. A. Intermittent drying of mango tissues: implementation of the reaction engineering approach (REA). *Ind. Eng. Chem. Res.* **2011**, *50*, 1089−1098.
(36) Putranto, A.; Chen, X. D.; Devahastin, S.; Xiao, Z.; Webley, P. A. Application of the reaction engineering approach (REA) to model intermittent drying under time-varying humidity and temperature. *Chem. Eng. Sci.* **2011**, *66*, 2149−2156.
(37) Putranto, A.; Chen, X. D.; Xiao, Z.; Webley, P. A. Mathematical modeling of convective and intermittent drying of rice and coffee using the reaction engineering approach (REA). *J. Food Eng.* **2011**, *105*, 638−646.
(38) Putranto, A.; Chen, X. D.; Xiao, Z.; Webley, P. A. Modeling of high-temperature treatment of wood by using the reaction engineering approach (REA). *Biores. Tech.* **2011**, *102*, 6214−6220.
(39) Putranto, A.; Chen, X. D.; Zhou, W. Modeling of baking of cake using the reaction engineering approach (REA). *J. Food Eng.* **2011**, *105*, 306−311.
(40) Kar, S.; Chen, X. D. Moisture transport across porcine skin: experiments and implementation of diffusion-based models. *Int. J. Healthcare Tech. Manage.* **2010**, *11*, 474−522.
(41) Kar, S.; Chen, X. D. Modeling of moisture transport across porcine skin using reaction engineering approach and examination of feasibility of the two phase approach. *Chem. Eng. Commun.* **2011**, *198*, 847−885.
(42) Putranto, A.; Chen, X. D. Spatial reaction engineering approach as an alternative for nonequilibrium multiphase mass transfer model for drying of food and biological materials. *AIChE J.* **2013**, *59*, 55−67.
(43) Kocaefe, D.; Younsi, R.; Poncsak, S.; Kocaefe, Y. Comparison of different models for the high-temperature heat-treatment of wood. *Int. J. Thermal Sci.* **2007**, *46*, 707−716.
(44) Chong, L. V.; Chen, X. D. A mathematical model of the self-heating of spray-dried food powders containing fat, protein, sugar and moisture. *Chem. Eng. Sci.* **1999**, *54*, 4165−4178.
(45) Incropera, F. P.; DeWitt, D. P. *Fundam. Heat Mass Transfer*; Wiley: New York, 2002.
(46) Van der Sman, R. G. M. Simple model for estimating heat and mass transfer in regular shaped foods. *J. Food Eng.* **2003**, *60*, 61−76.
(47) Microsoft Corp., http://office.microsoft.com/en-au/excel/ (accessed Mar 2012).
(48) Bird, R. B.; Stewart, W. E.; Lightfoot, E. N. *Transport Phenomena*, 2nd international ed.; John Wiley: New York, 2002.
(49) Slattery, J. C.; Bird, R. B. Calculation of the diffusion coefficient of dilute gases and of the self diffusion coefficient of dense gases. *AIChE J.* **1958**, *4*, 137−142.
(50) Audu, T. O. K.; Jeffreys, G. V. The drying of drops of particulate slurries. *Trans Inst. Chem. Eng. Part A* **1975**, *53*, 165−175.
(51) Gimmi, T.; Fuhler, H.; Studer, B.; Rasmuson, A. Transport of volatile chlorinated hydrocarbons in unsaturated aggregated media. *Water, Air Soil Pollut.* **1993**, *68*, 291−305.
(52) Madiouli, J.; Lecomte, D.; Nganya, T.; Chavez, S.; Sghaier, J.; Sammouda, H. A method for determination of porosity change from shrinkage curves of deformable Materials. *Drying Tech.* **2007**, *25*, 621−628.
(53) Chen, X. D., Mujumdar, A. S. *Drying Technologies in Food Processing*; Blackwell Publishing: U.K., 2008.
(54) Kar, S. *Drying of porcine skin-theoretical investigations and experiments*. Ph.D. thesis. Monash University, Australia. 2008.
(55) Chapra, S. C. *Numerical methods for engineers*; McGraw-Hill: Boston, 2006.
(56) Constantinides, A. *Numerical methods for chemical engineers with MATLAB applications*; Prentice Hall PTR: Upper Saddle River, NJ, 1999.
(57) Siau, J. F. *Transport Processes in Wood*; Springer-Verlag: Berlin, 1984.

(58) Simpson, W.; Tenwold, A. Physical properties and moisture relations of wood. *Wood Handbook*; USDA Forest Service, Forest Product Laboratory: Madison, WI; pp 1−23, 1999.